Ultrasonics Sonochemistry 94 (2023) 106336

Contents lists available at ScienceDirect

Ultrasonics Sonochemistry

journal homepage: www.elsevier.com/locate/ultson

Effects of ultrasonic-assisted pH shift treatment on physicochemical properties of electrospinning nanofibers made from rapeseed protein isolates

Yi-Ming Zhao [a,b,1], Yihe Li [a,b,c,1], Haile Ma [a,b], Ronghai He [a,b,*]

[a] School of Food and Biological Engineering, Jiangsu University, 301 Xuefu Road, Zhenjiang, Jiangsu, China
[b] Institute of Food Physical Processing, Jiangsu University, 301 Xuefu Road, Zhenjiang, Jiangsu, China
[c] College of Grain Engineering, Food & Drug, Jiangsu Vocational College of Finance & Economics, 8 Meicheng East Road, Huaian, Jiangsu, China

ARTICLE INFO

Keywords:
Rapeseed protein isolates
Electrospinning nanofibers
pH shift
Ultrasound
Physicochemical properties
Antibacterial activity

ABSTRACT

Electrospinning nanofibers (NFs) made from natural proteins have drawn increasing attention recently. Rapeseed meal is a by-product that rich in protein but not fully utilized due to poor properties. Therefore, modification of rapeseed protein isolates (RPI) is necessary to expand applications. In this study, pH shift alone or ultrasonic-assisted pH shift treatment was adopted, the solubility of RPI, along with the conductivity and viscosity of the electrospinning solution were detected. Moreover, the microstructure and functional characteristics of the electrospinning NFs, as well as the antibacterial activity of clove essential oil loaded-NFs were investigated. The tested parameters were remarkably improved after different treatments compared with the control, and synergistic effects were observed, especially under alkaline conditions. Hence, $pH_{12.5}$ + US showed the maximum value of solubility, conductivity, and viscosity, which was more than 7-fold, 3-fold, and almost 1-fold higher than the control respectively. Additionally, SEM and AFM images showed a finer and smoother surface of NFs after treatments, and the finest diameter of 216.7 nm was obtained after $pH_{12.5}$ + US treatment in comparison with 450.0 nm in control. FTIR spectroscopy of NFs demonstrated spatial structure changes of RPI, and improved thermal stability and mechanical strength of NFs were achieved after different treatments. Furthermore, an inhibition zone with a diameter of 22.8 mm was observed from the composite NFs. This study indicated the effectiveness of ultrasonic-assisted pH shift treatment on the physicochemical properties improvement and functional enhancement of NFs made from RPI, as well as the potential antibacterial application of the composite NFs in the future.

1. Introduction

Nanofibers (NFs) have attracted much attention in the past decade, and they have been widely studied in pharmaceutical, energy, food, and other fields due to their high specific surface area, simple preparation, and excellent mechanical properties [1,2]. Electrospinning is a novel and efficient technology for NFs fabrication. The instrument for electrospinning is mainly made up of a high-voltage power supply (either direct current or alternating current), a spinneret, a spinneret pump, and a collector of fibers. During electrospinning, the polymer solution is expressed from the spinneret by the syringe pump, and the solution is formed into liquid droplets due to surface tension. The droplets become charged under the high-voltage electric field, and electrostatic repulsion transforms the droplets into a Taylor cone, thus a charged jet is generated and ejected. The charged jet is stretched and elongated to a thinner diameter, which evaporates and solidifies quickly, producing a nanometer-scaled diameter of fibers on the collector with a range of 100–500 nm [3]. Electrospinning NFs have the potential to be used for food preservative, enzyme immobilization, food packaging, and other fields [4], which will bring huge economic benefits to the food industry. Many parameters, including processing parameters, liquid characteristics, and environmental factors can influence the structural morphology and diameter of the electrospinning NFs, thus further affecting the application of NFs [5,6]. Processing parameters mainly include applied voltage, liquid flow rate, and the distance between collector and spinneret. Liquid characteristics include concentration, viscosity,

* Corresponding author.
E-mail address: heronghai1971@126.com (R. He).
[1] Contributed equally to the study.

https://doi.org/10.1016/j.ultsonch.2023.106336
Received 13 December 2022; Received in revised form 12 February 2023; Accepted 13 February 2023
Available online 16 February 2023

conductivity, molecular weight, pH, etc. Major environmental factors include temperature and humidity. Therefore, research has been conducted to optimize the corresponding parameters in order to obtain NFs with excellent morphology and thinner diameters, as demonstrated by many studies [7–10].

Regarding electrospinning NFs preparation, increasing attention has been paid to eco-friendly biological material as public environmental awareness has increased. Proteins are a class of natural biological material that has been studied for NFs preparation, as reviewed by many researchers [11–13]. While proteins usually have poor spinnability and mechanical properties, hence the addition of other polymers is needed to improve the situation. Polyethylene oxide (PEO) is a water-soluble polymer with excellent mechanical performance, biocompatibility, and lower toxicity advantages. Importantly, PEO is quite electrospinnable due to high viscosity, thus the mixture of PEO with natural macromolecular substances can dramatically facilitate the spinnability of the solution. Therefore, PEO has been widely reported for electrospinning solutions preparation with other natural polymers, including soy protein isolate [14], whey protein isolate [15,16], keratin [17], alginates [18], chitosan [19,20], etc. Among them, Vega-Lugo et al. [15] reported that the viscosity of the electrospinning solution was increased when PEO was added to whey protein isolate, and bead-free NFs were obtained from the higher viscosity and lower surface tension under acidic conditions. Moreover, Dilamian et al. [21] prepared chitosan/PEO NFs in combination with poly (hexamethylene biguanide) hydrochloride (PHMB), and promising antibacterial activities of the composite NFs against *Escherichia coli* (*E.coli*) and *Staphylococcus aureus* (*S. aureus*) were observed, suggesting the potential application of PEO with other antimicrobial substances in the fabrication of biomaterials.

Rapeseed is one of the primary sources of vegetable oil attributed to its high yield [22]. Rapeseed meal is a by-product after oil extraction, and it was estimated to contain 40–45 % protein, while rapeseed meal is mainly utilized as animal feed or fertilizer due to poor solubility [23]. Therefore, various methods have been introduced to improve protein solubility and functional properties by modifying the molecular structure, and thus expand its applications [24]. Among them, pH shift and ultrasound technology are two of the most frequently investigated ones. pH shift is the process to treat proteins under extremely acidic or alkaline conditions with substantial adjustment to neutral pH, during which the structure and properties of proteins are changed. Many researchers have reported the influence of pH shift on protein solubility, hydrophobicity, emulsifying activity, etc, including whey protein isolate [25], pea protein [26], and soy protein isolate [27,28]. These studies demonstrated that pH shift is a relatively easy and effective modification method to enhance protein functionalities. Ultrasound is a green and non-thermal physical processing technology [29], which has also been extensively employed for protein modification [30–33]. These previous studies concluded that ultrasound can destroy the hydrogen bond and electrostatic force of protein via the cavitation effect, thus affecting the solubility, emulsion, foaming, and gelation properties of proteins. Apart from a single treatment, the combined treatment of pH shift and ultrasound has been drawing increasing attention recently, and synergistic effects have been reported [34–37]. For example, Li et al. [38] investigated the influence of ultrasonic-assisted pH shift with different treatment orders and ultrasound frequencies (fixed or sweep) on the modification of rapeseed protein isolates (RPI). Results showed that simultaneous treatment of ultrasound and pH shift led to higher solubility than sequential order. Meanwhile, decreased particle size, increased zeta potential, as well as changes in surface hydrophobicity, and content of free sulfhydryl were observed after the combined treatment. Moreover, Fourier transform infrared (FTIR) and fluorescence spectroscopy illustrated the spatial structure changes of proteins after treatments, demonstrating effectiveness of ultrasonic-assisted pH shift treatment on RPI modification.

Although electrospinning NFs made from proteins with bioactive materials have been studied before, to the best of our knowledge, NFs made from modified rapeseed protein with PEO, especially with natural antibacterial substance of the composite NFs have not been studied. To fill the gap, we carried out this study. RPI was pretreated by either a single pH shift or an ultrasonic-assisted pH shift. The solubility of RPI, as well as the conductivity and viscosity of the electrospinning solution made from the mixture of RPI and PEO were evaluated. Scanning electron microscopy (SEM), atomic force microscope (AFM), and FTIR were conducted to observe the microstructure of the NFs after different treatments. Meanwhile, the thermal stability and mechanical strength of the NFs were determined. Based on the detected parameters, the optimal treatment was selected to prepare the NFs that loaded with clove essential oil, and the antibacterial activity of the composite NFs against *E.coli* was tested.

2. Materials and methods

2.1. Materials and reagents

Rapeseed meal (38.5 % crude protein) was provided by COFCO-EOG Co., ltd. (Jiangsu, China). Polyethylene oxide (PEO) was ordered from Sigma Chemical Company (MO, USA). Acetone and potassium bromide (KBr) was purchased from Sinopharm Chemical Reagent Company (Shanghai, China). All the reagents employed were of analytical grade.

2.2. Rapeseed protein isolates (RPI) preparation

The extraction of RPI was conducted based on the protocol of Qu et al [39]. The rapeseed meal was crushed and passed through a 60 mesh sieve, then it was mixed with 75 % ethanol at a ratio of 1:5 (w/v). The mixture oscillated at room temperature for 20 min, followed by centrifugation (TGL-16, Changsha Xiangyi Centrifuge Instrument Company, Hunan, China) at 3,150 *g* for 15 min, and the precipitation was collected. This step was repeated twice to get rid of phenolics before extraction, and the extraction of RPI was based on the alkaline dissolution and acidic precipitation method. The pretreated rapeseed meal was lixiviated twice at 50 ℃ using an alkaline solution (pH 12.0) at a ratio of 1:15 (w/v) for 1 h each time, followed by centrifugation at 3,150 *g* for 15 min to collect the supernatant. The pH of the supernatant was then adjusted to 6.0 using 2.0 mol/L HCl with subsequent centrifugation of 3,150 *g* for 15 min, and the precipitation was collected. While the pH of the upper supernatant was adjusted to 3.6 with 2.0 mol/L HCl, and centrifugated (3,150 *g*, 15 min) to collect the precipitation again. The precipitation obtained twice was mixed and dissolved in distilled water with pH adjusted to neutral before dialyzing at 4 ℃ for 1 h. The dialysate was freeze-dried (ALPHA1-2, Martin Christ Inc, Germany) to obtain the final RPI (with 80.78 % protein) and stored at 4 ℃ for later usage.

2.3. Treatment of RPI

2.3.1. Single pH shift treatment

pH shift treatment was conducted according to Jiang et al [40] with minor modifications. RPI was dissolved with 100 mL distilled water and stirred at room temperature for 30 min with a final concentration of 25 mg/mL. The pH of the solution was adjusted to 1.5 or 12.5 with either 2 mol/L HCl or NaOH and kept stable (1 h, room temperature) to allow the unfolding of the protein chain. Following that, the pH of the solution was adjusted to a neutral pH of 7.0 using 2 mol/L NaOH or HCl, thus enabling the re-folding of the protein chain (1 h, room temperature).

2.3.2. Ultrasonic-assisted pH shift treatment

Regarding the combined treatment, 25 mg/mL RPI solution was transferred to an ultrasonic bath reactor (developed by Jiangsu University) and treated for 1 h immediately after being adjusted to the set pH value (1.5 or 12.5). The sonication parameters were chosen according to our earlier study [38,41] with the ultrasonic frequency of 28 kHz, and power of 40 W/L. The treatment was carried out at 40 ℃ for 30

min, and both pulse on-time and off-time was 3 s. After sonication, the following steps were the same as described in 2.3.1.

2.3.3. Labels of the different treatments in this study

As shown in Table 1, RPI solution either treated by pH shift alone or the combined ultrasound and pH shift was labeled in this study, and the solution (25 mg/mL) without any treatment was regarded as control. After treatment, the resultants were freeze-dried as described before and stored at 4 ℃ for subsequent analysis.

2.4. Solubility of RPI solution

The solubility of RPI was examined based on Jiang et al [36] with minor modifications. A 1.0 mL of the supernatant was transferred into a tube after centrifugation (3,150 *g*, 15 min), followed by the addition of 5.0 mL Folin reagent A. After a thorough shake, the solution was water-bathed at 30 ℃ for 10 min, with the subsequent addition of 1.0 mL Folin reagent B. Shook the mixture thoroughly and treated it in a water bath again (30 ℃, 10 min). The absorption of the solution was obtained at 500 nm with a UV spectrophotometer (Unic 7200, Unocal Corporation, Shanghai, China). The standard curve was plotted using bovine serum albumin. The solubility (%) was calculated as the proportion of soluble RPI to the total initial protein.

2.5. Electrospinning solution preparation

RPI was dissolved with 20 mL distilled water and made into a 5 mg/mL solution, followed by a medium-speed stir (room temperature, 30 min) on a magnetic stirrer (MSP-5E, Shanghai Kexing Instrument Co., ltd. China). Subsequently, 3 % (w/w) PEO was added into the solution and the mixture was stirred at high speed for 1 h, then changed to medium speed and continually stirred overnight to achieve a thorough mixture, and thus a colorless and transparent electrospinning solution was prepared.

2.6. Conductivity and viscosity of the electrospinning solution

A conductivity meter (DDS-307A, INESA Group Co., ltd. Shanghai, China) was adopted to determine the conductivity of the electrospinning solution. The viscosity was detected with a rheometer (HAAKEMARS III, Thermo Fisher Scientific Co., ltd. China) in the rotated mode. Lamina mold (C35/1°) was selected, and the share rate and temperature was 0.1–100 s^{-1} and 25 ℃, respectively. All the tests were completed within 24 h of the electrospinning solution preparation.

2.7. Electrospinning NFs preparation

An electrospinning setup (SNAN-01, Fukuoka, Japan) was used to generate electrospun NFs. A blunt-tipped needle of 0.5 mm (inner diameter) was selected, and 5 mL of electrospinning solution was transferred into a syringe. The syringe was placed on a syringe pump, and the solution was extruded from the spinneret at a flow rate of 2 mL/h. The supplied voltage was 22 kV, and the distance between the collector and the tip of the spinneret was 15 cm. Tin foil was attached to the metal plate to collect the NFs. When finished, the foil was placed in a vacuum-drying oven at 55 °C overnight, and subsequently transferred to a dryer for later use.

Table 1
Description of the treatments subjected to RPI solutions.

Treatment	Description
Control	Without any treatment
$pH_{1.5}$	pH shifted to 1.5
$pH_{12.5}$	pH shifted to 12.5
$pH_{1.5}$ + US	pH shifted to 1.5 + US treatment
$pH_{12.5}$ + US	pH shifted to 12.5 + US treatment

US parameters: frequency of 28 kHz, power of 40 W/L, temperature of 40 ℃, 30 min (both pulsed on-time and off-time was 3 s).

2.8. Scanning electron microscopy (SEM) of electrospinning NFs

The sample was fixed with double-sided conductive tape, and the surface was sprayed with a thin gold layer of 10 nm. The morphology of the NFs was obtained using a scanning electron microscope (S-3400 N, Hitachi High Tech, Japan) under the acceleration voltage of 15 kV.

2.9. Atomic force microscope (AFM) of electrospinning NFs

The AFM was conducted according to Hong et al [42] with some modifications. NFs was placed on the surface of a polished silicon wafer and dried in an incubator at 25 °C for 4 h. An atomic force microscope (MFP-3D, Asylum Res. Inc., USA) was used, and tapping mode was selected to obtain the topography of the sample. The diameter of the NFs was detected with the Bruker offline software (Nanoscope Analysis 1.5, Bruker Inc., Karlsruhe, Germany).

2.10. Fourier transform infrared (FTIR) spectroscopy of electrospinning NFs

FTIR spectroscopy of the NFs was carried out based on Xu et al. [43]. The prepared NFs were cut into pieces and mixed with overnight-dried KBr at a ratio of 1:100, the mixture was made into a slice of 1–2 mm. The spectroscopy was observed using an FTIR spectrometer (Nicolet IS50, Thermo Electron Corporation, USA) during 400–4000 cm^{-1} at a resolution of 4 cm^{-1}, and the KBr spectrum was used as background calculation. Omnic 8.0 software (Thermo Fisher Scientific Inc. Waltham, MA) and PeakFit 4.12 software (SPSS Inc., Chicago, IL, USA) were selected to analyze the FTIR spectral data.

2.11. Thermal stability of electrospinning NFs

The sample of 5–10 mg was placed in a crucible and loaded into a thermal gravimetric analyzer (TGA, Q50, Mettler Toledo Co., ltd. China). In the beginning, nitrogen was filled into the reaction chamber at 100 mL/min to expel air, and the temperature was increased from 35 °C to 600 °C at a rate of 10 °C/min. The results were analyzed with instrumental software.

2.12. Mechanical strength of electrospinning NFs

The electrospinning NFs were cut into small pieces with 2 × 6 cm (width × length) after preparation, and then the mechanical strength was detected by using a texture property analyzer (TPA, ST-Z16, Shangdong Shengtai Instrument Co., ltd. China). The initial distance between the fixtures was 50 mm and the stretching speed was 50 mm/min.

2.13. Antibacterial effect of electrospinning NFs-loaded essential oil

To study the potential of RPI electrospinning NFs as a carrier to load the antibacterial substance, RPI was treated under optimal conditions based on the aforementioned parameters. Clove essential oil (99 % purity, Florial Commercial & Trading Co., ltd. Shanghai, China) was mixed into the RPI solution with a concentration of 8 mg/mL to make the composite electrospinning NFs. The prepared NFs were aseptically cut into small pieces (10 × 10 mm) and exposed to UV light for 60 min before subsequent use. *E. coli* (ATCC25922) stored in our lab was selected as the target strain, and 200 μL of 1 × 10^6 CFU/mL of the bacterial suspension was inoculated to the nutrient agar (NA, Baisi biotech, Co., ltd. Hangzhou, China) plate and spread evenly. The inoculated plate was air-dried in the laminar flow cabinet for 10 min to allow

full absorption of the bacterial suspension, then the NFs piece was placed aseptically using a sterilized tweezer in the middle of the plate and incubated at 37 °C for 48 h to observe the inhibition zone. The NFs without clove essential oil were used as control.

2.14. Statistical analysis

The data were presented as the mean of three replicates ± standard deviation. The statistical analysis was performed using SPSS (IBM Cooperation, Chicago, USA), and the data were subjected to one-way analysis of variance (ANOVA) at the significant level of $P < 0.05$. Pearson Correlation analysis between solubility, conductivity, and diameter of the NFs was conducted by SPSS as well.

3. Results and discussion

3.1. Solubility of RPI

Solubility is a key factor influencing the functional properties of the protein, and thus affect the applications [44]. As shown in Table 2, the solubility of RPI after either single or combined treatment was significantly improved compared to the control ($P < 0.05$), especially under alkaline conditions. For instance, the solubility increased from 9.68 % (control) to 33.13 % after $pH_{12.5}$ treatment. Meanwhile, a synergistic effect of pH shift and ultrasound was observed compared to single pH shift treatment, with the value further increased to 81.19 % after $pH_{12.5}$ + US treatment, which was more than 7-fold higher than the control. The increase in solubility after pH shift treatment was due to the unfolding of protein structure under extremely acidic or alkaline conditions, which enabled more polar groups to get exposed, and thus improved the solubility. Jiang et al. [27] reported up to a 2.5-fold increase in soy protein isolate solubility after pH_{12} shift treatment, and similar results were also reported by other researchers [25,28,45,46]. Moreover, the lower solubility of RPI at $pH_{1.5}$ than at $pH_{12.5}$ may be attributed to the closer to the isoelectric point, where proteins have the lowest solubility. Regarding the synergistic effect of the combined treatment, the cavitation effect of ultrasound could disrupt the interactive force between proteins, including hydrogen bonding, Van de Waals forces, and dipole attractions, which led to more exposure of hydrophobic clusters and more release of protein molecules into the solution, hence the solubility was further enhanced. The synergistic effects of pH shift and ultrasound on solubility were also revealed in other plant or animal-based proteins. For instance, the solubility of milk casein concentrate was significantly increased from 59.02 % (control) to 99.05 % after ultrasound-assisted pH_{12} treatment [47]. Meanwhile, the solubility of pea protein isolates increased from 8.17 % (control) to 57.28 % after ultrasound-assisted pH_{10} treatment, while the value was only 9.80 % after a single pH_{10} treatment [36].

Table 2
Solubility, conductivity, and diameter of RPI, electrospinning solution, and electrospinning NFs respectively after different treatments.

Sample	PEO	Control	$pH_{1.5}$	$pH_{12.5}$	$pH_{1.5}$ + US	$pH_{12.5}$ + US
Solubility (%)	NA	9.68 ± 0.56^{a}	19.88 ± 0.79^{b}	33.13 ± 0.92^{d}	31.77 ± 0.98^{c}	81.19 ± 1.03^{e}
Conductivity (μs/cm)	130.4 ± 4.3^{a}	188.6 ± 15.4^{b}	444.8 ± 10.1^{c}	505.0 ± 5.2^{e}	489.0 ± 1.3^{d}	537.0 ± 13^{f}
Diameter (nm)	NA	450.0 ± 10.0^{f}	396.3 ± 25.2^{e}	316.7 ± 12.4^{c}	312.5 ± 21.7^{c}	216.7 ± 25.0^{a}

Note: NA means not available.
Different lower letters in the same row indicate significant difference at the level of $P < 0.05$.

3.2. Conductivity and viscosity of electrospinning solution

Conductivity is determinant to the charge to move to the surface of the droplet, which affects the formation of an electrostatic repulsion force. Therefore, conductivity is one of the important factors that could effectively reduce the surface tension of electrospinning solution, and thus has a great influence on the property of electrospinning solution. As can be seen from Table 2, the PEO solution had the lowest conductivity value, while the addition of RPI showed significantly increased conductivity ($P < 0.05$), and pH shift or the combined treatment further increased the value, especially combined treatment. Meanwhile, similar to solubility, the alkaline condition was more effective to increase conductivity than the acidic condition. For example, the conductivity of PEO was 130.4 ± 4.3 μs/cm, and the value was significantly increased to 444.8 ± 10.1 and 505.0 ± 5.2 μs/cm for $pH_{1.5}$ and $pH_{12.5}$ respectively ($P < 0.05$), and the maximum value of 537.0 ± 13 μs/cm was observed after $pH_{12.5}$ + US treatment. The increase in conductivity was mainly because the quantity of negative electric charge on the surface of the modified rapeseed protein increased, causing an increase in the charge of the electrospinning solution compared with the PEO solution. Therefore, the amount of electric charge passing through per unit area increased when the solution was in a high-voltage electric field, which increased the conductivity. Similar to our study, Vega-Luga et al. [15] also reported a higher conductivity value of whey protein isolate under alkaline conditions than acidic conditions, which was attributed to the large presence of OH^- ions.

Adequate viscosity plays a prominent role in the spinnability of electrospinning solution [48]. As shown in Fig. 1, when the shear rate increased, the apparent viscosity of all spinning solutions gradually decreased, which corresponds to the shear thinning property of non-Newtonian fluids. Moreover, the viscosity of the solution after combined treatment was higher than that after single pH shift treatment under all the shear rates, and the alkaline condition resulted in higher viscosity than the acidic condition, showing a similar trend to solubility. This is mainly due to that the electrospinning solution with higher solubility has a stronger molecular force and binding capability, thus the spatial structure of the protein is not easy to be destroyed when subjected to external forces, which leads to higher viscosity. Therefore, the maximum viscosity of 0.26 Pa.s (when 1/s was 0) was observed after $pH_{12.5}$ + US treatment in comparison with 0.14 Pa.s (when 1/s was 0) for control. Similarly, Vega-Lugo et al. [15] also reported increased viscosity in whey protein isolate after pH shift treatment, and Jiang et al. [49] observed higher viscosity values in more alkaline conditions for whey protein isolate as well.

3.3. SEM of electrospinning NFs

As can be seen from Fig. 2, there are certain differences in the appearance and diameter of NFs by different treatment methods. The NFs of control had a rough surface with beads and the largest diameter, and the fibers became finer after pH shift treatment. Meanwhile, the combined treatment led to the finest NFs with smooth surfaces, especially under alkaline conditions. The finer diameter of NFs has a higher specific surface area and porosity, which makes it easier to release the loaded substances as a carrier. In addition, the finer diameter can also increase the density of the fibers, leading to higher mechanical strength, thus finer diameter of NFs is always preferred. The diameter of the fibers was analyzed with Image J software according to the SEM image, and the results are shown in Table 2. As PEO solution cannot be well-formed into silk and exist in the form of a sheet, the diameter of the NFs was not available, while the mixture of RPI and PEO enabled the solution to form into NFs easier. The diameter of NFs in control was 450.0 ± 10.0 nm, which was significantly thicker than all the other samples ($P < 0.05$), and $HS_{12.5}$ + US showed the lowest value of 216.7 ± 25.0 nm. Similarly, a finer diameter of NFs in the alkaline condition than acidic condition was also observed by other researchers [15].

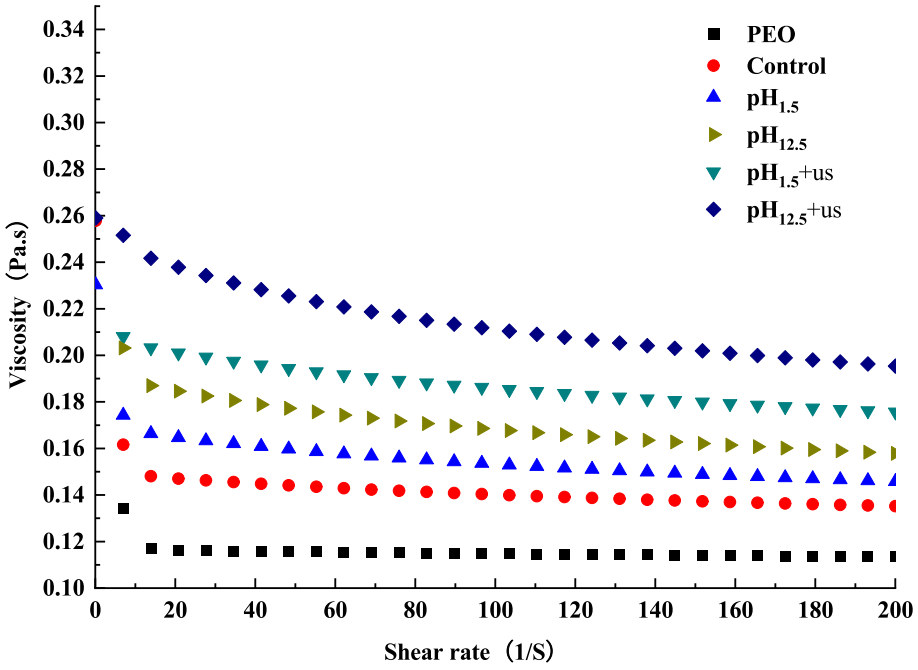

Fig. 1. The changes in viscosity under different shear rate of the electrospinning solutions after different treatments.

The difference in the NFs was due to the property of the electrospinning solution. As shown in Table 3, the diameter value was in significant negative correlation with solubility and conductivity values ($P < 0.01$). That is, an electrospinning solution with higher solubility and conductivity values resulted in finer and smoother surfaces of NFs. This can be ascribed to that a solution with higher conductivity can carry more electric charge, therefore subject to greater tensile force in a high-voltage electric field, thus forming a finer fiber structure. While it should be noted that if the conductivity of an electrospinning solution is too high, the solution will become unstable under the action of strong electric field force, which can lead to uneven fiber diameter.

Regarding the relationship between NFs diameter and viscosity, when a solution is spun in a high-voltage electrostatic field, the solution tends to form spherical droplets due to the surface tension, while a solution with high viscosity can overcome the surface tension effectively, to avoid or reduce the formation of beads on NFs. Besides, when the viscosity is high, more hydrogen bonds can be formed between proteins and polymers, resulting in a finer diameter and smoother surface of NFs. When the viscosity is not high enough, the NFs will be subjected to the action of surface tension, and thus beads will be formed.

3.4. AFM of electrospinning NFs

Fig. 3 presents the AFM of the NFs after different treatments. As shown in Fig. 3A, the NFs surface of the control was rough with large beads, demonstrating a poor spinning effect. After pH shift treatment, the NFs surface was improved and the beads became smaller (Fig. 3B&C). Moreover, the situation was further improved with fewer beads observed after the combined treatment (Fig. 3D&E). Additionally, the spinning effect of RPI under alkaline conditions was more promising than acidic conditions. The results were consistent with the conductivity and viscosity trend of the electrospinning solution after different treatments.

3.5. FTIR spectroscopy of electrospinning NFs

FTIR spectroscopy can reflect the protein molecular structure changes according to the vibration of functional groups at different wavelengths [50]. The three characteristic absorption bands of protein and corresponding wavelengths are as follows: amide I (C═O vibration, 1600–1700 cm^{-1}), amide II (N—H vibration, 1530–1550 cm^{-1}), and amide III (C═N vibration, 1260–1300 cm^{-1}), therefore the structural changes of protein can be analyzed by the three bands [51,52]. As shown in Fig. 4, for the control, there was a C═O vibration peak at the wavelength of 1,632 cm^{-1}, an N—H vibration peak at the wavelength of 1,538 cm^{-1}, and a C═N vibration peak at the wavelength of 1,230 cm^{-1}. After pH shift treatment or the combined treatment, the vibration peak of amide band II and amide band III was transferred to 1,540 and 1,238 cm^{-1} respectively, which suggested that more protein was unfolded, thus more amide acid got exposed. This phenomenon was mainly attributed to the influence of the interaction between protein and solvent [53]. Meanwhile, the stretching vibration peak of O—H and C—H at the wavelength of 3,405 and 2,923 cm^{-1} was transferred to 3,411 and 2,925 cm^{-1} respectively after combined treatment [54]. While regarding single pH shift treatment, the vibration peak of O—H did not change, just C—H transferred from 2,923 to 2,925 cm^{-1} under $pH_{12.5}$ treatment. The results indicated that combined treatment led to a more effective influence on protein structure changes than single pH shift treatment, which was in agreement with the properties of the electrospinning solution as discussed in section 3.2. Similar results have been revealed by Sun et al. [55]. FTIR analysis demonstrated that the functional groups of rapeseed protein have changed after different treatments, thus improving the binding strength. Among them, hydrogen bonds might play a vital role in the interaction, making the binding between protein and polymer more firmly [56], which was also reflected on the mechanical strength of NFs in section 3.7.

3.6. Thermal stability of electrospinning NFs

TGA is normally used to analyze the thermal stability of materials. The weight loss range of the NFs was primarily between 360 and 420 °C, with less weight loss in the early stage (Fig. 5). The weight loss between 35 and 105 °C was mainly due to water and volatiles evaporation, which accounted for 4–6 %. The weight loss of NFs under acidic conditions was less than that under alkaline conditions in the early stage, indicating the moisture content of NFs under acidic conditions was less. Fig. 4B shows that the maximum degradation rate temperature of control was 394.7 ℃, while the temperature was increased after all the treatments, and the

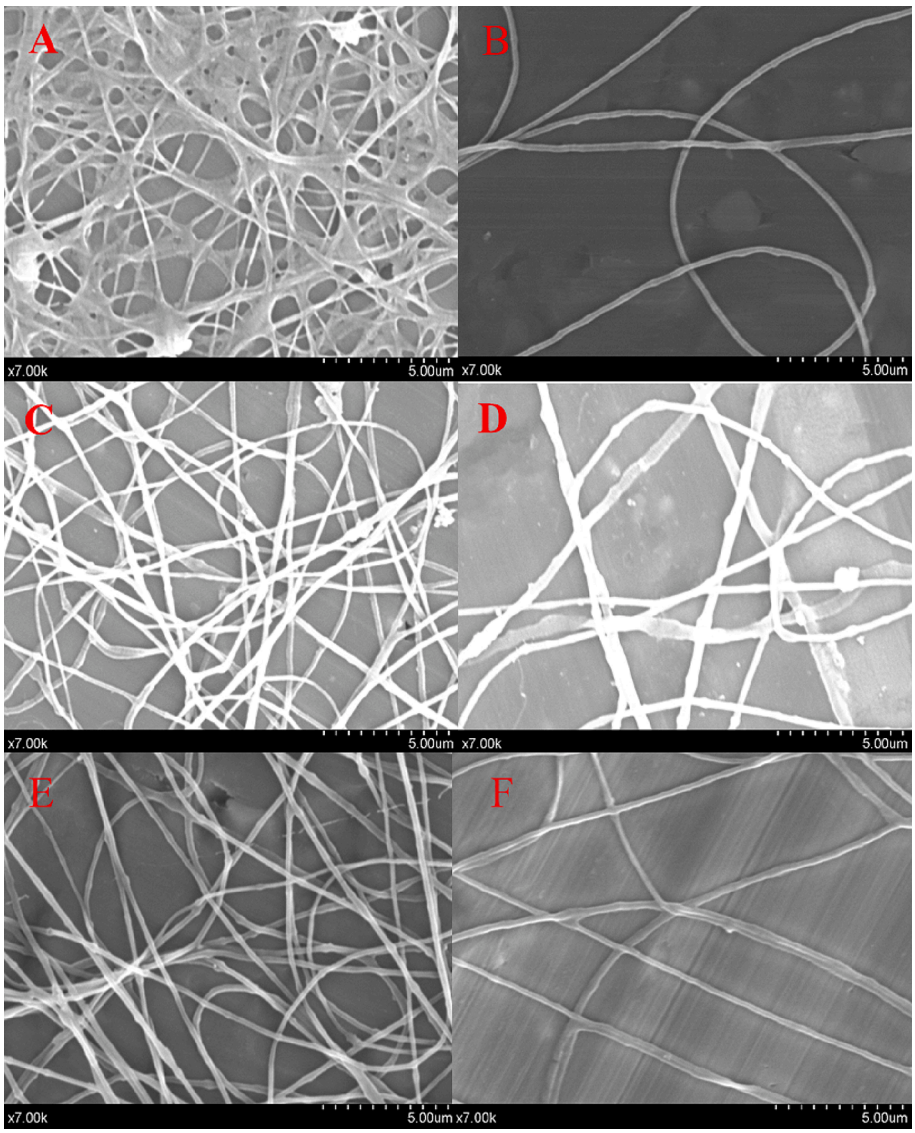

Fig. 2. SEM of electrospinning NFs after different treatments. (A) PEO; (B) Control; (C) $pH_{1.5}$; (D) $pH_{12.5}$; (E) $pH_{1.5}$ + US; (F) $pH_{12.5}$ + US.

Table 3
Pearson correlation coefficient between solubility, conductivity and diameter.

Parameter	Solubility	Conductivity	Diameter
Solubility	1		
Conductivity	0.680**	1	
Diameter	−0.934**	−0.839**	1

Note: ** indicates significantly correlated at the level of $P < 0.01$.

alkaline condition led to a higher rise than the acidic one. This was mainly attributed to the increased flexibility of rapeseed protein after alkaline treatment, and the molecular structure became loose, which can be tightly bound with PEO, and thus the thermal stability was higher than that under acidic conditions. Similar to our study, Jiang et al. [27] also reported increased thermal stability of soy protein isolate after pH shift treatment, especially under alkaline conditions. Regarding the decreased thermal stability after combined treatment, this may be because the structure of NFs treated with ultrasonic-assisted pH shift treatment was smoother, which reduced the bind of rapeseed protein with PEO, hence the thermal stability was decreased compared with single pH shift treatment. While opposite to our study, Sun et al. [55] reported increased thermal stability of coconut milk protein after combined pH shift and ultrasound treatment, especially under alkaline conditions. This may be attributed to different protein properties and different treatment conditions.

3.7. Mechanical strength of electrospinning NFs

Fig. 6 shows the mechanical strength of the NFs after different treatments. The overall trend demonstrated that the maximum stress was increased, while the rupture time was decreased except after $pH_{1.5}$ + US treatment. The control has the lowest maximum stress with a value of 105.9 g, but the rupture time of 11 s demonstrated promising elasticity, implying weak anti-destruction ability and strong tensile ability. The maximum stress of the NFs increased to 419.4 g and 640.7 g after $pH_{1.5}$ and $pH_{12.5}$ treatment respectively. While the elasticity of the NFs was decreased, with the rupture time dropped to 7.5 s (acidic condition) and 7.4 s (alkaline condition) respectively. Regarding the combined treatment, the maximum stress was 454.7 g after $pH_{1.5}$ + US treatment, with the largest rupture time of 13.5 s. Meanwhile, $pH_{12.5}$ + US treatment obtained the highest value of 809.8 g, with a rupture time of 8.5 s. The results suggested that the mechanical properties of NFs were improved after treatments, which could be due to the modification of the molecular structure of RPI. For instance, Jiang et al. [57] reported up to

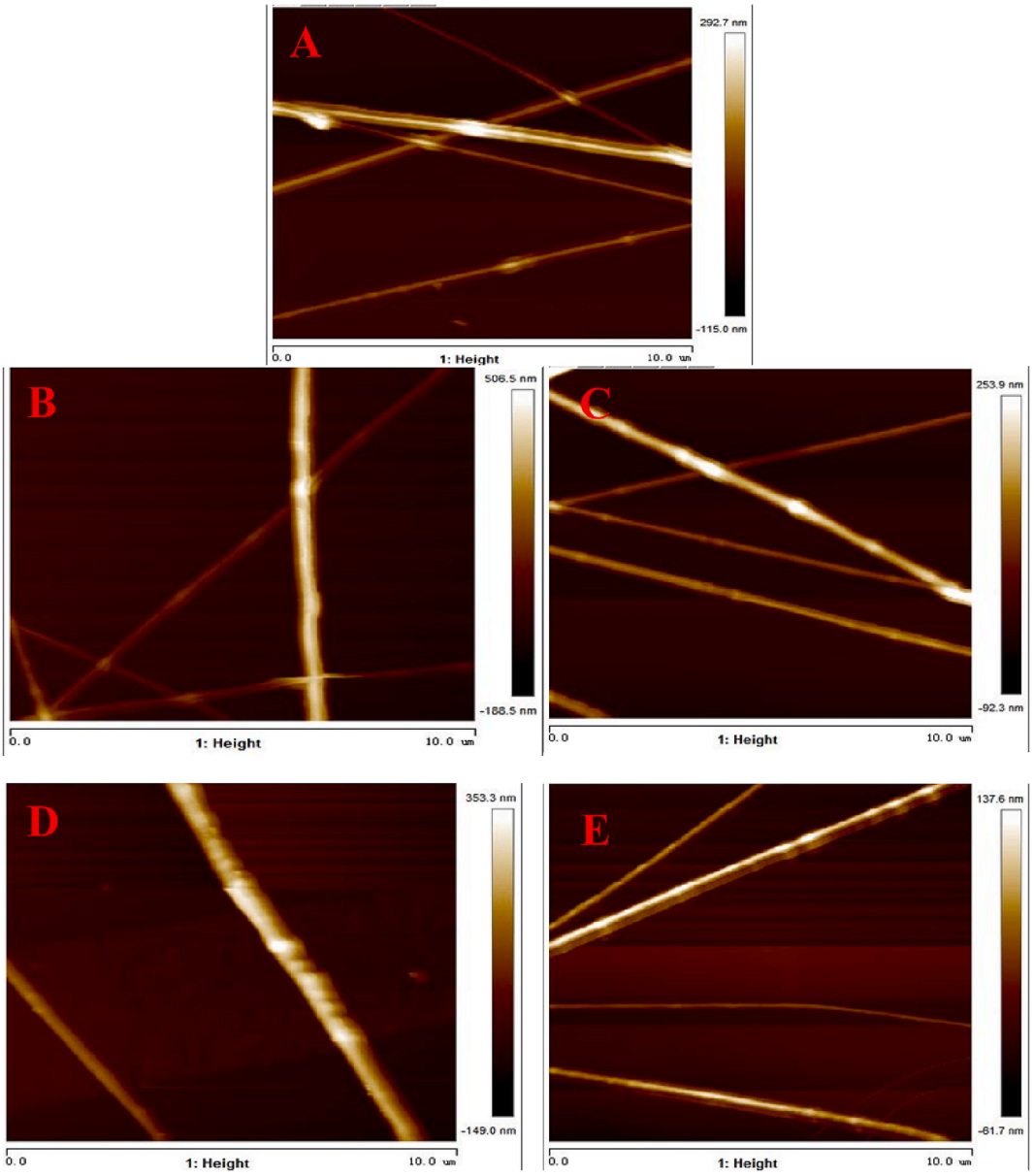

Fig. 3. AFM of electrospinning NFs after different treatments. (A) Control; (B) $pH_{1.5}$; (C) $pH_{12.5}$; (D) $pH_{1.5}$ + US; (E) $pH_{12.5}$ + US.

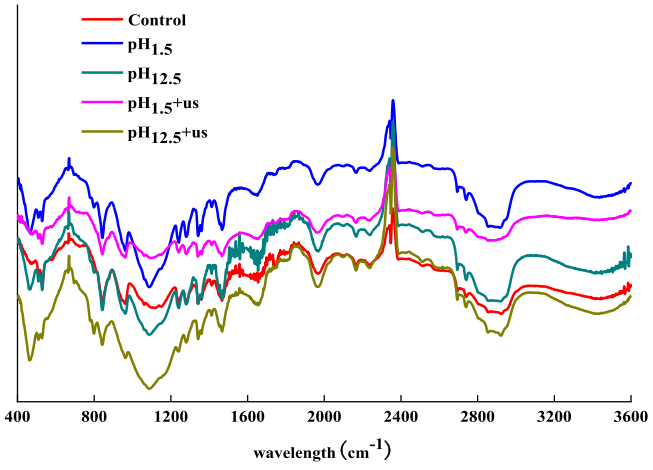

Fig. 4. FTIR of electrospinning NFs after different treatments.

2-fold greater elongation at the break of the film made from soy protein isolation after pH shift treatment than the control without any treatment. The increase of the maximum stress may be attributed to the generation of hydrogen bonds after treatments (as presented from FTIR analysis in section 3.5), resulting in firmer binding of protein and polymers [58]. Meanwhile, the flexibility of RPI was increased after treatments, especially under alkaline conditions (as reflected on thermal stability in section 3.6), which also contributed to the tighter binding of polymers. Therefore, $pH_{12.5}$ + US showed the highest maximum stress. Regarding the decreased rupture time, it may be due to the decreased diameter after treatments, as the finer diameter of NFs is more easily to be ruptured.

3.8. Antibacterial effect of electrospinning NFs-loaded essential oil

According to the preliminary analysis, RPI was treated by the optimal method of $pH_{12.5}$ + US, and the mixture of RPI and clove essential oil was made into NFs for the antibacterial test. There was no inhibition zone exhibited for NFs without clove essential oil (Fig. 7A),

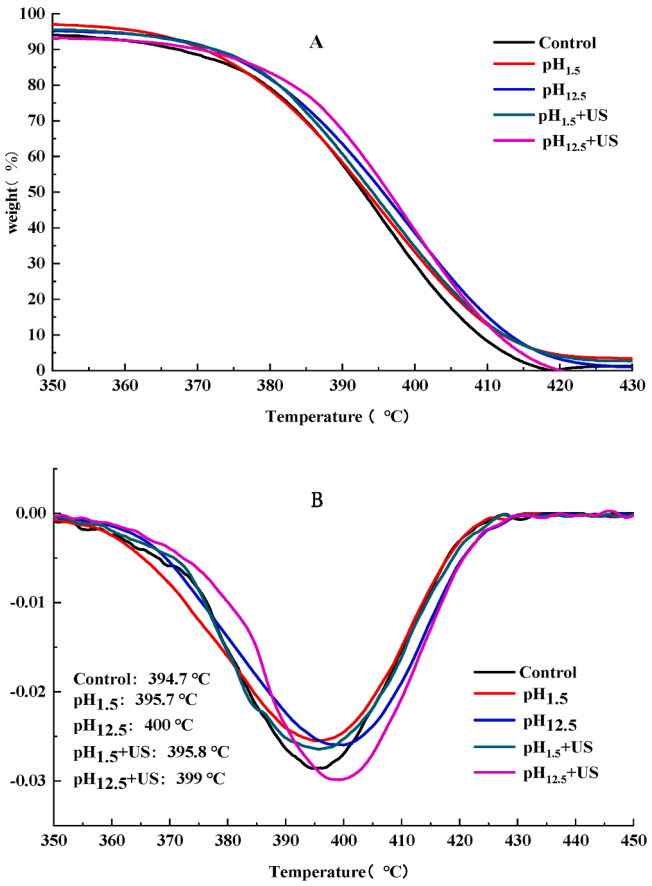

Fig. 5. Thermal stability of electrospinning NFs after different treatments. (A) Mass weight of NFs under different temperatures; (B) The second derivative diagram of NFs under different temperatures.

suggesting no antibacterial activity. While an inhibition zone with a diameter of 22.8 mm was observed when clove essential oil was loaded in the NFs (Fig. 7B). The results proved that antibacterial substance could act in the rapeseed protein NFs membrane, indicating the potential usage of rapeseed protein NFs to load antibacterial substances, and thus applied as antibacterial packing material in the agri-food industry in the future. Similarly, He et al. [59] evaluated the antimicrobial activity of silver nanoparticles (AgNPs)-embedded feather keratin (FK)/poly (vinylalcohol)/PEO composite NFs against *E. coli* (Gram-negative bacterium) and *S. aureus* (Gram-positive bacterium), and increasing antibacterial activity was observed with the increased amount of AgNPs. Moreover, the antibacterial activities of *Colocasia esculenta* tube protein-coated chitosan were also reported by Wardhani et al [60]. All of these studies demonstrated the potential expanded application of protein-based NFs.

4. Conclusions

This study was to investigate the physicochemical properties of electrospinning NFs made from RPI after single pH shift or ultrasonic-assisted pH shift treatment. Results showed that solubility, conductivity, and viscosity were significantly increased compared with the control ($P < 0.05$), and conductivity values were in positive correlation with solubility after different treatments. Meanwhile, synergistic effects of the combined treatment were observed, especially under alkaline conditions. Moreover, SEM and AFM demonstrated that the appearance of the NFs was improved after different treatments, and the finest NFs were obtained from $pH_{12.5}$ + US treatment with a smooth and bead-free surface. The diameter of the NFs was in negative correlation with solubility and conductivity. FTIR presented the spatial structure changes of the proteins in NFs after different treatments, which implied the closer bond of rapeseed protein with PEO. Thermal stability and mechanical strength of NFs were also improved after either single or combined treatments. Furthermore, the antibacterial activity of NFs-loaded clove essential oil was observed. In conclusion, the physicochemical properties of electrospinning NFs made from RPI were dramatically improved after ultrasonic-assisted pH shift treatment, and the composite NFs-loaded essential oil has the potential to be used for food preservation. While more work needs to be done in the future, including the

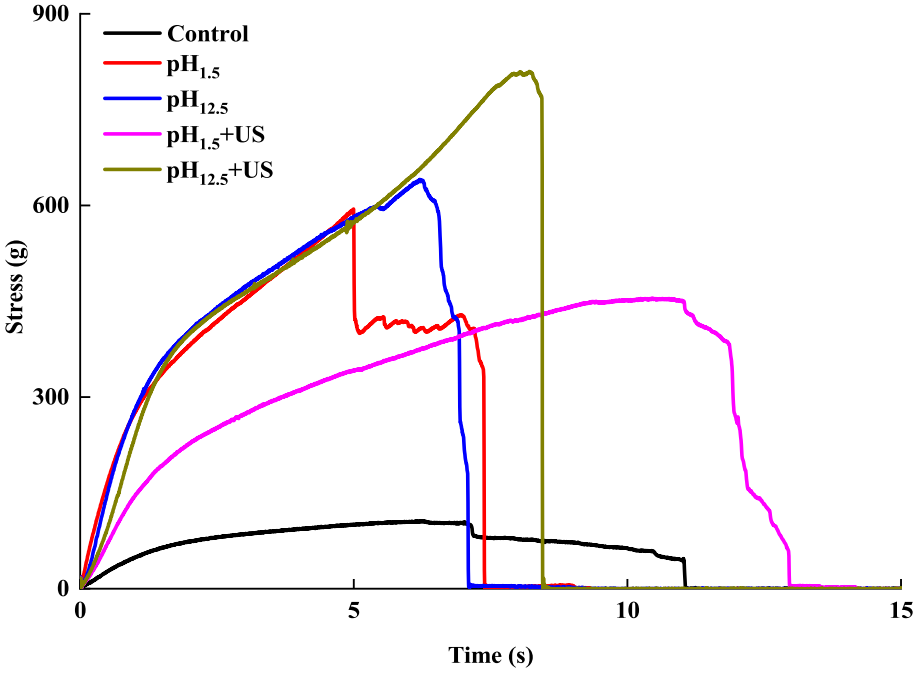

Fig. 6. Mechanical strength of electrospinning NFs after different treatments.

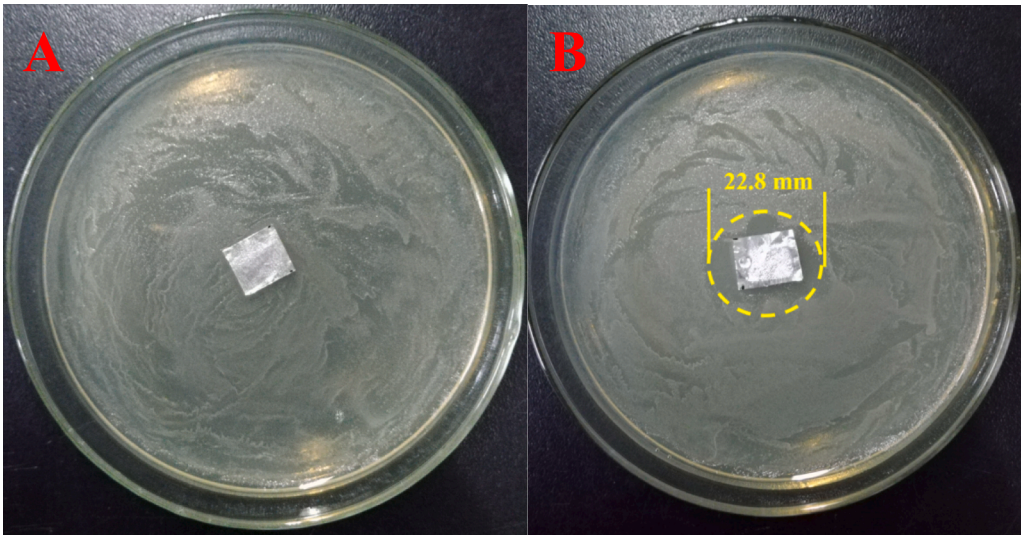

Fig. 7. Antibacterial effect of NFs against *E. coli*. (A) NFs without clove essential oil; (B) Clove essential oil-loaded NFs.

antimicrobial effect of the composite NFs against Gram-positive bacteria, the release kinetics of the essential oil, and the effectiveness of the composite NFs as a packing material on the shelf-life of food.

CRediT authorship contribution statement

Yi-Ming Zhao: Conceptualization, Methodology, Data curation, Writing – original draft, Funding acquisition. **Yihe Li:** Conceptualization, Methodology, Formal analysis. **Haile Ma:** Visualization, Supervision. **Ronghai He:** Conceptualization, Supervision, Writing – review & editing.

Declaration of Competing Interest

The authors declare that they have no known competing financial interests or personal relationships that could have appeared to influence the work reported in this paper.

Data availability

Data will be made available on request.

Acknowledgments

The authors would like to acknowledge the financial support of the National Natural Science Foundation of China (32202227), the Key Research & Develop plan of Shandong Province (2022CXGC010603), and the Senior Talent Program of Jiangsu University (5501360012).

References

[1] J. Sharma, et al., Multifunctional Nanofibers towards Active Biomedical Therapeutics, Polymers 7 (2) (2015) 186–219.
[2] S. Thenmozhi, et al., Electrospun nanofibers: New generation materials for advanced applications, Materials Science and Engineering B-Advanced Functional Solid-State Materials 217 (2017) 36–48.
[3] P.R. Patel, R.V.N. Gundloori, A review on electrospun nanofibers for multiple biomedical applications, Polymers for Advanced Technologies (2022).
[4] Kumar, T.S.M., et al., *A comprehensive review of electrospun nanofibers: Food and packaging perspective.* Composites Part B-Engineering, 2019. **175**.
[5] Wei, L., et al., *Influence of the processing parameters on needleless electrospinning from double ring slits spinneret using response surface methodology.* Journal of Applied Polymer Science, 2018. **135**(27).
[6] J. Chen, et al., Review of the Principles, Devices, Parameters, and Applications for Centrifugal Electrospinning, Macromolecular Materials and Engineering 307 (8) (2022).
[7] L.R. Manea, et al., Mathematical Model of the Electrospinning Process II. Effect of the technological parameters on the electrospun fibers diameter, Revista De Chimie 67 (8) (2016) 1607–1612.
[8] A.H. Hekmati, et al., Effect of needle length, electrospinning distance, and solution concentration on morphological properties of polyamide-6 electrospun nanowebs, Textile Research Journal 83 (14) (2013) 1452–1466.
[9] V. Jacobs, A. Patanaik, R.D. Anandjiwala, Optimization of Process and Solution Parameters in Electrospinning Polyethylene Oxide, Advanced Science Letters 4 (11–12) (2011) 3590–3595.
[10] V. Jacobs, R.D. Anandjiwala, M. Maaza, The Influence of Electrospinning Parameters on the Structural Morphology and Diameter of Electrospun Nanofibers, Journal of Applied Polymer Science 115 (5) (2010) 3130–3136.
[11] M.D.P. Pereira da Cunha, P. Christian Caracciolo, G. Abel Abraham, *Latest advances in electrospun plant-derived protein scaffolds for biomedical applications.* Current Opinion, Biomedical Engineering (2021) 18.
[12] A.C. Mendes, K. Stephansen, I.S. Chronakis, Electrospinning of food proteins and polysaccharides, Food Hydrocolloids 68 (2017) 53–68.
[13] Y. Wang, et al., Electrospinning of Natural Biopolymers for Innovative Food Applications: A Review, Food and Bioprocess Technology (2022).
[14] X. Xu, et al., Preparation and Properties of Electrospun Soy Protein Isolate/Polyethylene Oxide Nanofiber Membranes, Acs Applied Materials & Interfaces 4 (8) (2012) 4331–4337.
[15] A.-C. Vega-Lugo, L.-T. Lim, Effects of poly(ethylene oxide) and pH on the electrospinning of whey protein isolate, Journal of Polymer Science Part B-Polymer Physics 50 (16) (2012) 1188–1197.
[16] J. Colin-Orozco, et al., Properties of Poly (ethylene oxide)/whey Protein Isolate Nanofibers Prepared by Electrospinning, Food Biophysics 10 (2) (2015) 134–144.
[17] H. Ma, et al., Fabrication of wool keratin/polyethylene oxide nano-membrane from wool fabric waste, Journal of Cleaner Production 161 (2017) 357–361.
[18] M. Castellano, et al., Electrospun composite mats of alginate with embedded silver nanoparticles: Synthesis and characterization, Journal of Thermal Analysis and Calorimetry 137 (3) (2019) 767–778.
[19] M. Fadaie, et al., Stabilization of chitosan based electrospun nanofibers through a simple and safe method, Materials Science and Engineering C-Materials for Biological Applications 98 (2019) 369–380.
[20] S. Abid, et al., Enhanced antibacterial activity of PEO-chitosan nanofibers with potential application in burn infection management, International Journal of Biological Macromolecules 135 (2019) 1222–1236.
[21] M. Dilamian, M. Montazer, J. Masoumi, Antimicrobial electrospun membranes of chitosan/poly(ethylene oxide) incorporating poly(hexamethylene biguanide) hydrochloride, Carbohydrate Polymers 94 (1) (2013) 364–371.
[22] M.D.M. Yust, et al., Rapeseed protein hydrolysates: a source of HIV protease peptide inhibitors, Food Chemistry 87 (3) (2004) 387–392.
[23] Y. Yoshie-Stark, Y. Wada, A. Waesche, Chemical composition, functional properties, and bioactivities of rapeseed protein isolates, Food Chemistry 107 (1) (2008) 32–39.
[24] F.U. Akharume, R.E. Aluko, A.A. Adedeji, Modification of plant proteins for improved functionality: A review, Comprehensive Reviews in Food Science and Food Safety 20 (1) (2021) 198–224.
[25] W. Chen, et al., Effect of pH-shifting treatment on structural and functional properties of whey protein isolate and its interaction with (-)-epigallocatechin-3-gallate, Food Chemistry 274 (2019) 234–241.
[26] H.-N. Liang, C.-h., Tang, *pH-dependent emulsifying properties of pea Pisum sativum (L.) proteins*, Food Hydrocolloids 33 (2) (2013) 309–319.
[27] J. Jiang, Y.L. Xiong, J. Chen, pH Shifting Alters Solubility Characteristics and Thermal Stability of Soy Protein Isolate and Its Globulin Fractions in Different pH,

Salt Concentration, and Temperature Conditions, Journal of Agricultural and Food Chemistry 58 (13) (2010) 8035–8042.
[28] Q. Liu, et al., Structural and Gel Textural Properties of Soy Protein Isolate When Subjected to Extreme Acid pH-Shifting and Mild Heating Processes, Journal of Agricultural and Food Chemistry 63 (19) (2015) 4853–4861.
[29] Y. Tao, et al., Bridge between mass transfer behavior and properties of bubbles under two-stage ultrasound-assisted physisorption of polyphenols using macroporous resin, Chemical Engineering Journal 436 (2022).
[30] H. Hu, et al., Effects of ultrasound on structural and physical properties of soy protein isolate (SPI) dispersions, Food Hydrocolloids 30 (2) (2013) 647–655.
[31] X. Yang, et al., Effects of ultrasound pretreatment with different frequencies and working modes on the enzymolysis and the structure characterization of rice protein, Ultrasonics Sonochemistry 38 (2017) 19–28.
[32] T. Xiong, et al., Effect of high intensity ultrasound on structure and foaming properties of pea protein isolate, Food Research International 109 (2018) 260–267.
[33] C. Hong, et al., Effects of dual-frequency slit ultrasound on the enzymolysis of high-concentration hydrolyzed feather meal: Biological activities and structural characteristics of hydrolysates, Ultrasonics Sonochemistry 89 (2022).
[34] S. Li, et al., Effects of ultrasound and ultrasound assisted alkaline pretreatments on the enzymolysis and structural characteristics of rice protein, Ultrasonics Sonochemistry 31 (2016) 20–28.
[35] H. Lee, et al., Soy protein nano-aggregates with improved functional properties prepared by sequential pH treatment and ultrasonication, Food Hydrocolloids 55 (2016) 200–209.
[36] S. Jiang, et al., Modifying the physicochemical properties of pea protein by pH-shifting and ultrasound combined treatments, Ultrasonics Sonochemistry 38 (2017) 835–842.
[37] L. Huang, et al., Changes in the structure and dissociation of soybean protein isolate induced by ultrasound-assisted acid pretreatment, Food Chemistry 232 (2017) 727–732.
[38] Y. Li, et al., Modification of rapeseed protein by ultrasound-assisted pH shift treatment: Ultrasonic mode and frequency screening, changes in protein solubility and structural characteristics, Ultrasonics Sonochemistry 69 (2020).
[39] W. Qu, et al., Effects of ultrasonic and graft treatments on grafting degree, structure, functionality, and digestibility of rapeseed protein isolate-dextran conjugates, Ultrasonics Sonochemistry 42 (2018) 250–259.
[40] J. Jiang, et al., Interfacial Structural Role of pH-Shifting Processed Pea Protein in the Oxidative Stability of Oil/Water Emulsions (vol 62, pg 1683, 2014), Journal of Agricultural and Food Chemistry 62 (18) (2014) 4225.
[41] Y. Li, et al., Inhibition Effect of Ultrasound on the Formation of Lysinoalanine in Rapeseed Protein Isolates during pH Shift Treatment, Journal of Agricultural and Food Chemistry 69 (30) (2021) 8536–8545.
[42] C. Hong, et al., Effects of dual-frequency slit ultrasound on the enzymolysis of high-concentration hydrolyzed feather meal: Biological activities and structural characteristics of hydrolysates, Ultrasonics Sonochemistry 89 (2022), 106135.
[43] B. Xu, et al., Effect of multi-frequency power ultrasound (MFPU) treatment on enzyme hydrolysis of casein, Ultrasonics Sonochemistry 63 (2020).
[44] C. Arzeni, et al., Comparative study of high intensity ultrasound effects on food proteins functionality, Journal of Food Engineering 108 (3) (2012) 463–472.
[45] J. Li, et al., Effect of pH-shifting treatment on structural and heat induced gel properties of peanut protein isolate, Food Chemistry 325 (2020).
[46] H. Dai, et al., Improvement of the solubility and emulsification of rice protein isolate by the pH shift treatment, International Journal of Food Science and Technology (2022).
[47] X. Zhao, et al., Modifying the physicochemical properties, solubility and foaming capacity of milk proteins by ultrasound-assisted alkaline pH-shifting treatment, Ultrasonics Sonochemistry 88 (2022).
[48] S.K. Tiwari, S.S. Venkatraman, Importance of viscosity parameters in electrospinning: Of monolithic and core-shell fibers, Materials Science & Engineering C-Materials for Biological Applications 32 (5) (2012) 1037–1042.
[49] L. Jiang, et al., Effect of acid/alkali shifting on function, gelation properties, and microstructure of Mesona chinensis polysaccharide-whey protein isolate gels, Food Hydrocolloids 117 (2021).
[50] S.W. Ellepola, S.M. Choi, C.Y. Ma, Conformational study of globulin from rice (Oryza sativa) seeds by Fourier-transform infrared spectroscopy, International Journal of Biological Macromolecules 37 (1–2) (2005) 12–20.
[51] D.M. Byler, H. Susi, Examination of the secondary structure of proteins by deconvolved FTIR spectra, Biopolymers: Original Research on Biomolecules 25 (3) (1986) 469–487.
[52] W.K. Surewicz, H.H. Mantsch, New insight into protein secondary structure from resolution-enhanced infrared spectra, Biochimica et Biophysica Acta (BBA)-Protein Structure and Molecular Enzymology 952 (1988) 115–130.
[53] Z. Wang, et al., Polyphenol-induced cellulose nanofibrils anchored graphene oxide as nanohybrids for strong yet tough soy protein nanocomposites, Carbohydrate Polymers 180 (2018) 354–364.
[54] E. Abraham, et al., Extraction of nanocellulose fibrils from lignocellulosic fibres: A novel approach, Carbohydrate Polymers 86 (4) (2011) 1468–1475.
[55] Y. Sun, et al., Effect of ultrasound on pH-shift to improve thermal stability of coconut milk by modifying physicochemical properties of coconut milk protein, Lwt-Food Science and Technology, 2022, p. 167.
[56] M.M. Demir, et al., Electrospinning of polyurethane fibers, Polymer 43 (11) (2002) 3303–3309.
[57] J. Jiang, et al., Structure-modifying alkaline and acidic pH-shifting processes promote film formation of soy proteins, Food Chemistry 132 (4) (2012) 1944–1950.
[58] A. Papadaki, et al., Tuning the physical and functional properties of whey protein edible films: Effect of pH and inclusion of antioxidants from spent coffee grounds, Sustainable Chemistry and Pharmacy (2022) 27.
[59] M. He, et al., Electrospun Silver Nanoparticles-Embedded Feather Keratin/Poly (vinyl alcohol)/Poly(ethylene oxide) Antibacterial Composite Nanofibers, Polymers 12 (2) (2020).
[60] R.A.K. Wardhani, et al., Physical-Chemical Crosslinked Electrospun Colocasia esculenta Tuber Protein-Chitosan-Poly (Ethylene Oxide) Nanofibers with Antibacterial Activity and Cytocompatibility, International Journal of Nanomedicine 15 (2020) 6433–6449.